Image-Based Bronchial Anatomy Codification for Biopsy Guiding in Video Bronchoscopy

Esmitt Ramírez[1][0000−0001−7573−631X], Carles Sánchez[1][0000−0003−3435−9882], Agnés Borràs[1][0000−0002−7747−9924], Marta Diez-Ferrer[2][0000−0002−0207−8157], Antoni Rosell[2][0000−0003−0877−7191], and Debora Gil[13][0000−0002−2770−4767]

[1] Computer Vision Center, Autonomous University of Barcelona 08193, Spain
{esmitt.ramirez, csanchez, agnesba, debora}@cvc.uab.es
[2] Bellvitge University Hospital, L'Hospitalet de Llobregat 08907, Spain
{marta.diez, arosell}@bellvitgehospital.cat
[3] Serra Húnter Fellow, Spain

Abstract. Bronchoscopy examinations allow biopsy of pulmonary nodules with minimum risk for the patient. Even for experienced bronchoscopists, it is difficult to guide the bronchoscope to most distal lesions and obtain an accurate diagnosis. This paper presents an image-based codification of the bronchial anatomy for bronchoscopy biopsy guiding. The 3D anatomy of each patient is codified as a binary tree with nodes representing bronchial levels and edges labeled using their position on images projecting the 3D anatomy from a set of branching points. The paths from the root to leaves provide a codification of navigation routes with spatially consistent labels according to the anatomy observes in video bronchoscopy explorations. We evaluate our labeling approach as a guiding system in terms of the number of bronchial levels correctly codified, also in the number of labels-based instructions correctly supplied, using generalized mixed models and computer-generated data. Results obtained for three independent observers prove the consistency and reproducibility of our guiding system. We trust that our codification based on viewer's projection might be used as a foundation for the navigation guidance in bronchoscopy-based systems.

Keywords: biopsy guiding, bronchoscopy, lung biopsy, intervention guiding, airway codification

1 Introduction

Suspicious pulmonary nodules might be diagnosed with a histopathologic analysis on a sample of biopsy tissue, which can be extracted in minimally invasive bronchoscopic examinations. A main restraint of flexible bronchoscopy is the difficulty to determine the best pathway to peripheral lesions. According to [1], physician's accuracy at defining proper 3D routes is only on the order of 40% for ROIs located near airways at fourth generation or less, with errors beginning as early as second generation.

Despite recent advances, a few novel endoscopy techniques seem to increase diagnostic yield to 70-80% and still radiate the patient. The diagnostic yield could be improved by reducing the radiation and costs and with the support of imaging technologies which may better guide the physician to the target lesion.

Virtual bronchoscopic (VB) systems [2] are used to reconstruct computed tomography (CT) data into three-dimensional representations of the tracheobronchial tree. VB systems allow for pairing virtual and real-time bronchoscopy, being useful for guiding ultrathin bronchoscopes and other devices in diagnostic interventions [3]. During exploration, indicating the planned path on the current intra-operative video could increase the intervention efficiency whereas reducing radiation to clinical staff. To accurately guide the operator across the planned path, assisted navigation, such as electromagnetic [4], radial probe ultrasound [5] or image-based virtual bronchoscopic navigation [6, 7], should identify in intra-operative videos the different airway levels that VB follows.

According to Khan [3], the main advantage of virtual bronchoscopic navigation (VBN) whether electromagnetic navigation or radial probe ultrasound is its lower cost including consumables. Furthermore, during the procedure, VBN might provide information on the airways in cases where video bronchoscopic frames do not display the tracheobronchial tree due to either blood, mucus or airway swelling. The main disadvantage of VBN is the lack to capture the real-time information about both 3D position and directional guidance from the operator point of view [3]. The codification of patient's airways 3D anatomy includes a labeling of the bronchial levels traversed across the navigation path. This can help the operator to identify the path to follow and, as consequence, to improve VBN intra-operative guidance.

The codification of patient's airways 3D anatomy is a main point in the development of a computer-assisted system for diagnosis, treatment planning, and follow-up of pulmonary diseases. Several works are concerned with the codification and matching for improving registration of 3D scans in assessment of obstructive pulmonary diseases. Airways 3D anatomy is usually described as a graph using the bifurcations and end-points of the segmentation skeleton [8]. The variability across acquisitions and patients, as well as, imperfections in segmentation and skeletonization introduce missing and spurious branches that hamper further matching and labelling of the constructed graphs. Usual solutions include pruning of small skeleton branches [9] or tree-matching strategies able to cope with topological changes [10, 11].

Concerning airways labeling, this process is mainly restricted to anatomical names identified by matching unlabeled airway trees to atlas-based labeled models. Even for methods successfully handling topological changes of the airway tree [12], anatomical labeling in human airway trees is well defined up to the segmental level. This restricts the number of labels to 20-32 bronchial segments [10], is a major inconvenience for distal navigation in biopsy guiding. A recent work [13] proved the feasibility of labeling at sub-segmental levels using spatial 3D information of branches.

In this paper, we present a graph-based codification of airways for guiding bronchoscopy interventions in lung cancer biopsy procedures. Contrasting other approaches, we use a graph structure to prune bifurcations introduced by imperfections in the segmentation and skeletonization. Our proposal uses geometrical aspects (i.e. branching levels) of the segmentation skeleton to obtain an appropriate codification for guiding. Also, we label the airways using their position in 2D images (quadrant-based approach), projected from the perspective of the viewer which is obtained from virtual VB explorations. As far as we know, this is the first work using virtual explorations to label airways according to their position in video-bronchoscopy 2D frames. We provide a sub-segmental personalized labeling to generate intuitive routing instructions for physicians.

2 Codification of Airways Navigation Paths

A navigation path across airways can be given by the sequence of the navigated bronchial levels labeled in such a way that the branch to follow is identified into intra-operative bronchoscopy videos. The complete structure of all bronchial levels is represented using a graph with nodes. This structure is defined by bronchial levels and edges labeled according to the position that bronchi would have in bronchoscopic explorations.

Airways are tubular structures with their geometry determined by the centerline given by bronchi lumen center. The airways centerlines correspond to the skeleton of segmented volumes, and they allow the construction of a tree-based structure on bronchi branching. The skeleton of a segmented volume is encoded using the Kerschnitzki et al. [14] approach, where a graph represents its branching geometry using nodes and edges. For instance, this approach was previously used to segment airways amongst match CT-videos bronchial structure with encoded airways, using landmarks in the anatomical structure [15, 16].

The nodes of the graph correspond to the skeleton branching points and its edges represent branch connectivity. The Depth-First Search (DFS) algorithm considers the trachea as the root node, and it allows directs the graph to depth levels; this allows associate a level for each of its nodes to define a binary rooted tree structure. DFS also defines the relationship parent/children each time a bronchi branch is found, being the bifurcations before skeleton end-points the leaves of the tree. This parent/children relationship lets encoding the tree structure using two adjacency matrices, see Fig. 1, for fast computing of graph operations (e.g. cycle detection, graph matching, maximum flow, and others). The first matrix represents the node tree connectivity in a binary matrix, and the second one is a matrix of 3D segments that keeps the list of 3D skeleton points (i.e. $(x, y, z) \in R^3$) that connect each pair of adjacent nodes. Each position in the matrix of 3D segments is composed by a list of equally spaced points.

Skeleton false branches that not belong at bronchial anatomy, introduce extra nodes in the graph structure that hinder the codification of bronchial levels. These branches correspond to intermediate nodes of first order (i.e. with only one child), in the adjacency matrix connecting two nodes, namely v_i, v_j, of

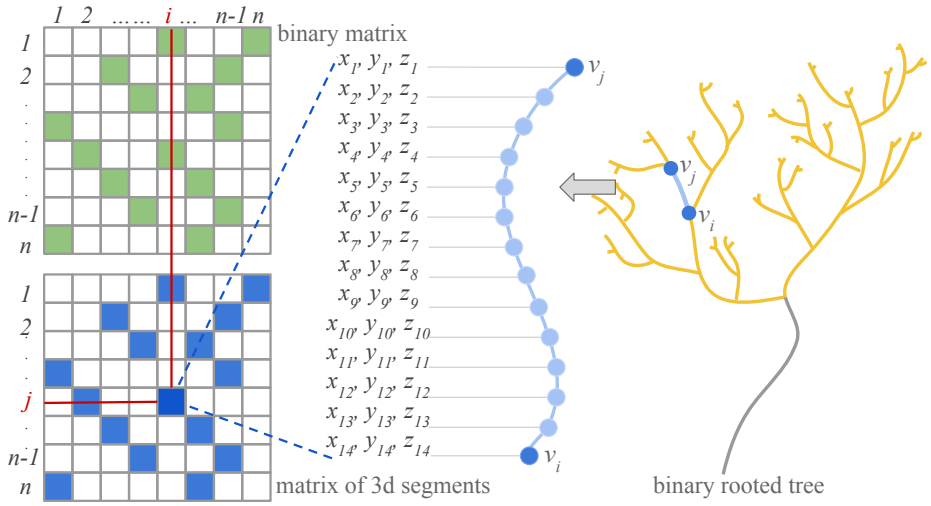

Fig. 1. Binary and segments matrices codifying airway anatomy as rooted tree. The colored positions in both matrices, represent the parent/children relationship.

different order (either a leaf or a node of order two). Intermediate nodes are deleted from the two adjacency matrices removing their rows and columns, and updating the position i, j with the adjacency information and the list of skeleton points connecting v_i, v_j.

A navigation route is defined as a node sequence $v_{k0}, v_{k1}, \ldots v_{kj-1}, v_{kj}$, connecting a leaf node (v_{kj}) with the root (v_{k0}). A final navigation path inside the segmented volume is the collection of skeleton 3D points extracted from the matrix of 3D segments by considering the entrances given by $(k0, k1), \ldots, (kj-1, kj)$. To provide an edge labeling consistent with intra-operative visual information, a navigation route was simulated. This route is created across the segmented volume and projects the segmented 3D geometry at each traversed bronchial level to obtain a collection of virtual images of the intra-operative path. The position of the projected bronchi in such virtual images provides our edge labeling for intuitive routing.

Then, in a navigation route, to each pair of consecutive nodes, v_{k-1}, v_k, a camera is placed in one of the skeleton points at a given distance d_k from the end node v_k. This distance permits capture the complete border of lumen's border for bifurcations. Next, the camera target point is set to v_k, and the up vector is accumulated during path traversal (i.e roll axis) using the FrenetSerret frame. Also, the camera field of view is set to 120° to ensure full visibility of geometry in virtual frames. Accordingly, d_k varies on each segment being set to $0.2 \times dist(v_{k-1}, v_k)$. The scene projected at each level is given by the following simplified representation of the essential bronchial 3D structure. We project two lines from v_k to its children nodes v^1_{k+1} and v^2_{k+1}, called $S1$ and $S2$ respectively. This allows a clear identification of the lines in virtual images, each projected

line has a different primary color, red and green. Thus, each line is codified in a different RGB channel.

To label each projected line, the virtual image is split into four quadrants centered at the projected position of v_k. Since quadrants represent the spatial distribution of airway lumens in bronchoscopic frames during traversal of bronchial levels, each projected segment will be labeled according to the quadrant it belongs to. Then for each point of the projected segment, the position of the quadrant they belong to is computed. For this, the mode and average values are considered. The mode indicates the predominant quadrant where each segment belongs. When two or three segments lie on the same quadrant, they are counterclockwise ordered according to their average.

The labeling process is described in the visual scheme shown in Fig. 2. Figure shows an outline of airways and a navigation path with its branching nodes labeled. The figure also displays a camera positioned at distance d_k from the node v_k, and the segments $S1$, $S2$ colored in red and green respectively. The rectangular images show the simplified scene projected over the complete airway anatomy. The most left image is split into four colored quadrants: Q_1=red, Q_2=green, Q_3=yellow, Q_4=blue, to illustrate that $S1$ lies in Q_1 and $S2$ in Q_2.

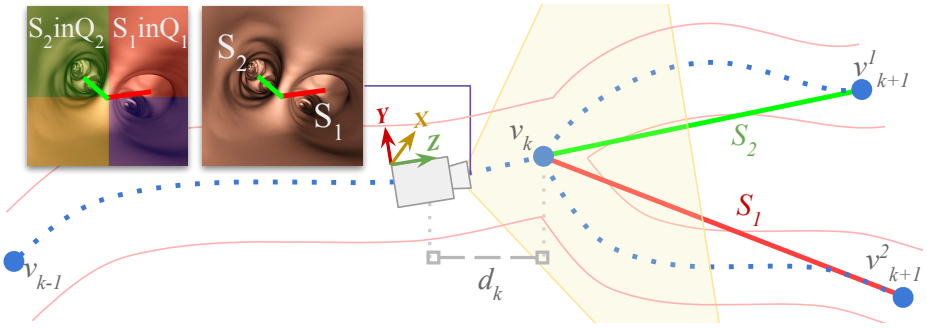

Fig. 2. Edge Labelling Procedure: the camera captures an image at distance d_k from the v_k, projecting lines to children at level $k+1$. Image is split into quadrants to label line segments S_1, S_2.

Using edge labels, navigation paths are encoded with a set of spatial instructions specified by the labels of the edges linking path nodes, Q_1-Q_3-Q_1-Q_2-Q_4. This agrees to route a path with instructions (up/right/left/down at every branch) which are natural for physicians [17]. Such instructions mean "at first bifurcation take the first quadrant, after the third, ..., and so on". Since these instructions are not intuitive to follow during an intervention, we replace quadrant names for upper-right, upper-left, lower-left and lower-right indicating each quadrant in a more natural language.

3 Experiments and Discussion

The capabilities of our labeling for bronchoscopy guiding were evaluated, mainly focus in two aspects: identification of the bronchial levels traversed, and validation of bronchi orientation in projected images as intuitive instructions for distal routing. To do so, a set of virtual explorations on CT volumes using an interactive simulation platform developed in Unity were developed.

For each CT-scan of a patient, four virtual explorations were generated, covering the four main lobes: left and right upper lobes, noted LUL, RUL, and left and right lower lobes, noted LLL, RLL. These paths were performed using the central navigation without rotation around the scope. For each path, a sequence of intuitive instructions (upper-left, upper-right, down-left, down-right) was extracted using our method. These instructions were validated by three experts who tried to reproduce the path in the simulation platform using the instructions supplied at each level detected by the graph. Experts were asked to identify instructions not corresponding to an actual branching level to define a false level rate (FLR). At each bifurcation where an expert could not reproduce the route previously simulated, was also recorded to define a false instruction rate (FIR).

Data were managed and evaluated through generalized mixed models using software R version 3.2.5. For each quality score (FLR, FIR), a different Poisson model was adjusted to include the segmental lobe as a factor. Moreover, a random subject effect to account for intra-individual variability among cases and a random effect to model inter-observer variability:

$$log(FIRijk) = \beta_0 + \beta_1 Lobe + Pat_i + Obs_j + \epsilon_{ijk}$$
$$log(FLRijk) = \beta_0 + \beta_1 Lobe + Pat_i + Obs_j + \epsilon_{ijk}$$

for $Pat_i \sim N(0, \sigma_{Pat})$ denoting the random effect that models intra-patient variability, $Obs_j \sim N(0, \sigma_{Obs})$ the random effect for inter-observer variability and *Lobe* (with values LUL, RUL, LLL, RLL) for the grouping factor of the four segmental lobes considered. Model assumptions were validated by means of residual analysis and influential values. The model coefficients, p values and 95% confidence interval (CI) for significance in main effects were also computed. The CIs values were back transformed to the original scale for their interpretation. Furthermore, a p value < 0.05 was considered statistically significant.

For our tests, ten cases were considered with paths reaching between the sixth and twelfth bronchial level. Descriptive statistics, for instance, the average and standard deviation (SD), also the model adjustment for both, FLR and FIR as percentage way, are shown in Table 1. There are not any significant differences across lung lobes for the rate of false detected levels with average overall values in the range 3 ± 7. Nevertheless, the lower left lung lobe has a significantly worse (p-val < 0.01) rate of false instructions with CIs equal to $(5.2, 20.6)\%$.

The increase in the FIR value for the lower left lung lobe is mainly due to the confusing instructions at the third generation, just after the LUL-LLL branching point. Although the 3D geometry around the third generation presents two branching points (thus, two levels), they are not appreciated in the projected

Table 1. Models for FLR and FIR.

	Descriptive		Model				Descriptive		Model		
FLR (%)	mean	SD	coeff	p-val	CI	FIR (%)	mean	SD	coeff	p-val	CI
RLL	0.0	0.0	1	-	(0.0,1.6)		2.8	4.6	1	-	(0.6, 5.2)
LLL	3.3	7.2	0.5	0.33	(0.0, 3.4)		13	11.7	1.3	<0.01	(5.2, 20.6)
RUL	1.8	3.5	0.4	0.4	(0.0, 3.0)		1.7	4.0	-0.35	0.06	(0.1, 3.4)
LUL	7.0	12.4	1.0	0.07	(0.0, 6.0)		6.4	8.7	0.64	0.08	(2.2, 10.5)

images due to a short distance between them. In fact, in projected images, the LLL lumen is not visually identified and three airway lumens that correspond to the projection of LLL next generation are visible. Therefore, from the point of view of the operator, there are three possible airways to follow at the same level, while for our codification there are two consecutive levels with two airways each.

Figure 3 illustrates this phenomenon. Whereas the 3D structure in front of the camera contains the segments $v_k \rightarrow v^1_{k+1}$ and $v_k \rightarrow v^2_{k+1}$ as well as v^1_{k+1} children segments $v^1_{k+1} \rightarrow v^1_{k+2}$ and $v^1_{k+1} \rightarrow v^2_{k+2}$, its projection shown in the right image only shows lumens corresponding to v^2_{k+1}, v^1_{k+2}, v^2_{k+2}. This visual artifact also occurs in intra-operative videos as the top image illustrates. The image shows a frame extracted at the same position from an exploration performed on the patient, which is used to generate the simulated image shown below.

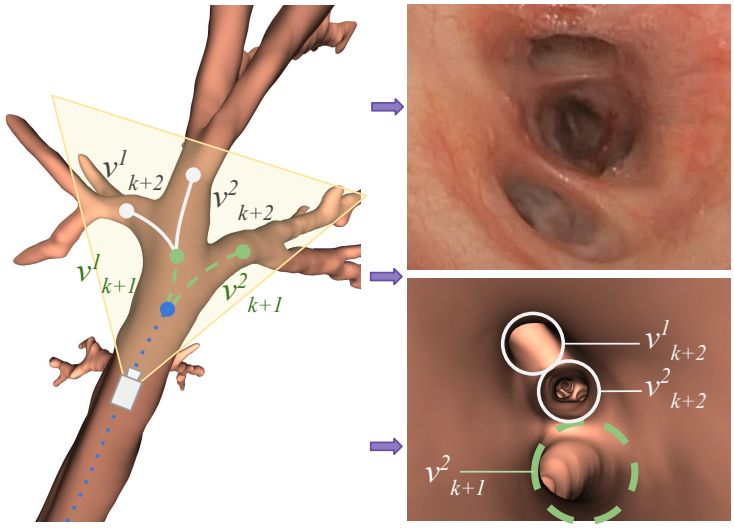

Fig. 3. System failure at spatially close bifurcations, where projections skip one of them and show three possible airways to follow.

4 Conclusions

We have introduced a codification of the bronchial anatomy, for biopsy guiding based on a symbolic representation of each patient's airway anatomy as a binary rooted tree. Tree nodes represent the bronchial levels, and their edges are labeled according to the position of bronchi in virtual video bronchoscopy. This provides to physicians a set of intuitive instructions during biopsy guiding.

Experiments on data simulating different routes to each pulmonary lobe allow the validation of our approach as a system for supplying instructions in biopsy guiding (with the successful average guiding of $94.7\% \pm 9.1\%$ in the cases). Also, we might correctly codify up to the tenth generation, forward of that, our segmentation approach needs some improvements. The statistical analysis detected a bias in instructions for the left lower lobe introduced by the spatially close consecutive levels, which are visualized as a single level with three lumens in the projected images. In such cases, the system should issue a single instruction instead of two. To avoid this phenomenon, the tree codification may be merged consecutive levels into a single level, considering the branching point distance).

Although this is an off-line validation with simulated data, we might conclude that a guiding system based on bronchi orientation in 2D projections is feasible and simple enough, and it might be easily deployed in operating rooms with low costs. The integration of this approach into an interactive navigation support system is currently under development [18], and we have the confidence to compare it with the LungPoint system in a near future.

Acknowledgments

This work was supported by Catalan, Spanish and European projects DPI2015-65286-R, 2014-SGR-1470, CERCA Programme / Generalitat de Catalunya. Also, the first author holds the fellowship number BES-2016-078042 granted by the Ministry of Economy, Industry and Competitiveness, Spain. Carles Sánchez is supported by the ACCIO Tecniospring TECSPR17-1-0045 Program. A Titan X Pascal was used for this research, donated by NVIDIA.

References

[1] Marina Y. Dolina, Duane C. Cornish, Scott A. Merritt, Lav Rai, Rickhesvar Mahraj, William E. Higgins, and Rebecca Bascom. Interbronchoscopist Variability in Endobronchial Path Selection: A Simulation Study. *Chest*, 133(4):897 – 905, 2008.

[2] Páll Jens Reynisson, Håkon Olav Leira, Toril A. Nagelhus Hernes, Erlend F. Hofstad, Marta Scali, Hanne Sorger, Tore Amundsen, Frank Lindseth, and Thomas Langø. Navigated bronchoscopy: a technical review. *Journal of bronchology & interventional pulmonology*, 21 3:242–64, 2014.

[3] Kashif Ali Khan, Pietro Nardelli, Alex Jaeger, Conor O'Shea, Padraig Cantillon-Murphy, and Marcus P. Kennedy. Navigational Bronchoscopy for Early Lung Cancer: A Road to Therapy. *Advances in Therapy*, 33(4):580–596, Apr 2016.

[4] Sandeep J. Khandhar, Mark R. Bowling, Javier Flandes, Thomas R. Gildea, Kristin L. Hood, William S. Krimsky, Douglas J. Minnich, Septimiu D. Murgu, Michael Pritchett, Eric M. Toloza, Momen M. Wahidi, Jennifer J. Wolvers, and Erik E. Folch. Electromagnetic navigation bronchoscopy to access lung lesions in 1,000 subjects: first results of the prospective, multicenter NAVIGATE study. *BMC Pulmonary Medicine*, 17(1):59, Apr 2017.

[5] Yasuyuki Ikezawa, Naofumi Shinagawa, Noriaki Sukoh, Megumi Morimoto, Hajime Kikuchi, Masahiro Watanabe, Kosuke Nakano, Satoshi Oizumi, and Masaharu Nishimura. Usefulness of Endobronchial Ultrasonography With a Guide Sheath and Virtual Bronchoscopic Navigation for Ground-Glass Opacity Lesions. *The Annals of Thoracic Surgery*, 103(2):470 – 475, 2017.

[6] Fumihiro Asano, Takashi Ishida, Naofumi Shinagawa, Noriaki Sukoh, Masaki Anzai, Kenya Kanazawa, Akifumi Tsuzuku, and Satoshi Morita. Virtual bronchoscopic navigation without X-ray fluoroscopy to diagnose peripheral pulmonary lesions: A randomized trial. *BMC Pulmonary Medicine*, 17:184, 12 2017.

[7] Ralf Eberhardt, Nicolas Kahn, Daniela Gompelmann, Maren Schumann, Claus Peter Heussel, and Felix J. F. Herth. LungPoint–a new approach to peripheral lesions. *Journal of thoracic oncology : official publication of the International Association for the Study of Lung Cancer*, 5 10:1559–63, 2010.

[8] L. Florez Valencia, A. Morales Pinzón, J.-C. Richard, M. Hernandez Hoyos, and M. Orkisz. Simultaneous skeletonization and graph description of airway trees in 3D CT images. In *XXVème Colloque GRETSI*, Lyon, France, September 2015.

[9] Duván Alberto Gómez Betancur, Anna Fabijańska, Leonardo Flórez-Valencia, Alfredo Morales Pinzón, Eduardo Enrique Dávila Serrano, Jean-Christophe Richard, Maciej Orkisz, and Marcela Hernández Hoyos. Airway segmentation, skeletonization, and tree matching to improve registration of 3d ct images with large opacities in the lungs. In Leszek J. Chmielewski, Amitava Datta, Ryszard Kozera, and Konrad Wojciechowski, editors, *Computer Vision and Graphics*, pages 395–407, Cham, 2016. Springer International Publishing.

[10] Alfredo Morales Pinzón, Marcela Hernández Hoyos, Jean-Christophe Richard, Leonardo Florez-Valencia, and Maciej Orkisz. A tree-matching algorithm: Application to airways in CT images of subjects with the acute respiratory distress syndrome. *Medical image analysis*, 35:101–115, 2017.

[11] C. Bauer, M. Eberlein, and R. R. Beichel. Airway tree reconstruction in expiration chest CT scans facilitated by information transfer from corresponding inspiration scans. *Medical Physics*, 43:1312–1323, March 2016.

[12] Aasa Feragen, Jens Petersen, Megan Owen, Pechin Lo, Laura Hohwu Thomsen, Mathilde Marie Winkler Wille, Asger Dirksen, and Marleen de Bruijne. Geodesic atlas-based labeling of anatomical trees: Application and evaluation on airways extracted from CT. *IEEE Transactions on Medical Imaging*, 34(6):1212–1226, 2015.

[13] Juerg Tschirren, Craig Vidal, Benjamin Baron, Philippe Raffy, and Eric Hoffman. Fully automated labeling of sub-segmental airways in human airway trees. *European Respiratory Journal*, 46:PA758, 09 2015.

[14] Michael Kerschnitzki, Philip Kollmannsberger, Manfred C Burghammer, Georg N. Duda, Richard Weinkamer, Wolfgang Wagermaier, and Peter Fratzl. Architecture of the osteocyte network correlates with bone material quality. *Journal of bone and mineral research : the official journal of the American Society for Bone and Mineral Research*, 28(8):1837–45, 2013.

[15] Antonio Esteban-Lansaque, Carles Sánchez, Agnés Borràs, Marta Diez-Ferrer, Antoni Rosell, and Debora Gil. Stable anatomical structure tracking for video-bronchoscopy navigation. In Raj Shekhar, Stefan Wesarg, Miguel Ángel González Ballester, Klaus Drechsler, Yoshinobu Sato, Marius Erdt, Marius George Linguraru, and Cristina Oyarzun Laura, editors, *Clinical Image-Based Procedures. Translational Research in Medical Imaging (CLIP-MICCAI)*, pages 18–26. Springer International Publishing, 2016.

[16] Carles Sánchez, Antonio Esteban-Lansaque, Agnés Borràs, Marta Diez-Ferrer, Antoni Rosell, and Debora Gil. Towards a videobronchoscopy localization system from airway centre tracking. In *12th International Conference on Computer Vision Theory and Applications (VISAPP)*, pages 352–359, 2017.

[17] Bronchoscopy International. What is Bronchoscopy Step-by-Step, 2018. https://bronchoscopy.org.

[18] Esmitt Ramírez, Carles Sánchez, Agnés Borràs, Marta Diez-Ferrer, Antoni Rosell, and Debora Gil. BronchoX: Bronchoscopy Exploration Software for Biopsy Intervention Planning. *Healthcare Technology Letters*, 2018. DOI: 10.1049/htl.2018.5074.